

REPORT DOCUMENTATION PAGE

Form Approved
OMB No. 0704-0188

Public reporting burden for this collection of information is estimated to average 1 hour per response, including the time for reviewing instructions, searching existing data sources, gathering and maintaining the data needed, and completing and reviewing this collection of information. Send comments regarding this burden estimate or any other aspect of this collection of information, including suggestions for reducing this burden to Department of Defense, Washington Headquarters Services, Directorate for Information Operations and Reports (0704-0188), 1215 Jefferson Davis Highway, Suite 1204, Arlington, VA 22202-4302. Respondents should be aware that notwithstanding any other provision of law, no person shall be subject to any penalty for failing to comply with a collection of information if it does not display a currently valid OMB control number. PLEASE DO NOT RETURN YOUR FORM TO THE ABOVE ADDRESS.

1. REPORT DATE (DD-MM-YYYY)

26-01-2009

2. REPORT TYPE

Final Technical Report

3. DATES COVERED (From - To)

May-Dec 2008

4. TITLE AND SUBTITLE

Reduced Power Laser Designation Systems

5a. CONTRACT NUMBER**5b. GRANT NUMBER**

N00178-08-1-9001

5c. PROGRAM ELEMENT NUMBER**6. AUTHOR(S)**

Barry G. Sherlock

5d. PROJECT NUMBER**5e. TASK NUMBER****5f. WORK UNIT NUMBER****7. PERFORMING ORGANIZATION NAME(S) AND ADDRESS(ES)**

University of North Carolina at Charlotte, 9201 University
City Boulevard, Charlotte, NC 28223

**8. PERFORMING ORGANIZATION REPORT
NUMBER****9. SPONSORING / MONITORING AGENCY NAME(S) AND ADDRESS(ES)**

Naval Surface Warfare Center
Dahlgren Laboratory
17320 Dahlgren Road
Dahlgren, VA 22448-5100

10. SPONSOR/MONITOR'S ACRONYM(S)

NSWC

**11. SPONSOR/MONITOR'S REPORT
NUMBER(S)****12. DISTRIBUTION / AVAILABILITY STATEMENT**

Approved for public release; distribution is Unlimited.

13. SUPPLEMENTARY NOTES

None.

14. ABSTRACT

This work contributed to the Micropulse Laser Designation (MPLD) project. The objective of MPLD is to develop a 6-lb eye-safe micro-pulse laser system to locate, identify, range, mark, and designate stationary and moving targets. MPLD presents a range of new circuit design and signal processing problems, and the present work addressed some of these problems. Work done includes: investigating techniques for increasing photodiode preamplifier bandwidth and reducing photodiode preamplifier noise; calculation of visibility angles for laser designation in urban environments; investigating the use of a negative impedance converter circuit to reduce the effect of the photodiode capacitance; investigating a two-transistor circuit for bootstrap buffering of the input stage; comparing the noise performance of the candidate amplifier designs; selection of the two-transistor bootstrap design as the circuit of choice; and comparing the performance of this circuit against that of a basic transconductance amplifier.

15. SUBJECT TERMS

Laser Guided Weapons; Laser designation; laser rangefinders; infrared photodiodes; transconductance amplifiers.

16. SECURITY CLASSIFICATION OF:

a. REPORT
U

b. ABSTRACT
U

c. THIS PAGE
U

**17. LIMITATION
OF ABSTRACT**

UU

**18. NUMBER
OF PAGES**

14

19a. NAME OF RESPONSIBLE PERSON
B.G. Sherlock

**19b. TELEPHONE NUMBER (include area
code)**
704-687-2722

Final Report on NSWC Grant N00178-08-1-9001

Title: Reduced Power Laser Designation Systems

PI: Barry Sherlock
University of North Carolina at Charlotte
Charlotte, NC 28023
Phone (704)687-2722 Fax: (704)687-2352
email: sherlock@uncc.edu

Date: January 10, 2009

I. Introduction

This work contributes to the Micropulse Laser Designation (MPLD) project. The objective of this project is to develop a 6-lb eye-safe micro-pulse laser system to locate, identify, range, mark, and designate stationary and moving targets.

MPLD uses laser pulses of much lower energy and higher repetition rates than in existing laser designation systems. Because of this, MPLD presents a range of new circuit design and signal processing problems, and the present work seeks to address some of these problems.

This work involved the design of a photodiode preamplifier suitable for use in the MPLD project, by investigating techniques for increasing photodiode amplifier bandwidth, and reducing photodiode amplifier noise.

II. Narrative and Research Accomplishments

This report covers the research accomplishments for the entire period of the grant, and therefore repeats the material from the monthly progress reports for the first two months of the project.

II.1 Background

A photodiode can be modeled as a current source in parallel with a capacitance, as illustrated in Figure 1.

20090202019

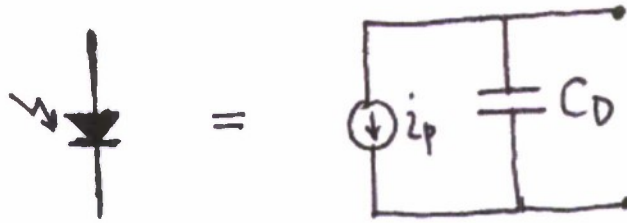


Figure 1. Photodiode equivalent circuit.

The photodiode envisaged for the present system has capacitance $C_D = 225$ pF. Since the signal has a bandwidth of about 3 MHz and a gain of about 1000 is desired, this presents formidable problems to the circuit designer. Because of the low power of the laser pulses, the amplitude of the input signal is very small, and therefore a further important consideration is to minimize the noise of the circuit. Unfortunately, photodiode amplifiers have very complex noise response.

The appropriate amplifier for a photodiode is a current-to-voltage amplifier (transconductance amplifier), the basic form of which is illustrated in Figure 2.

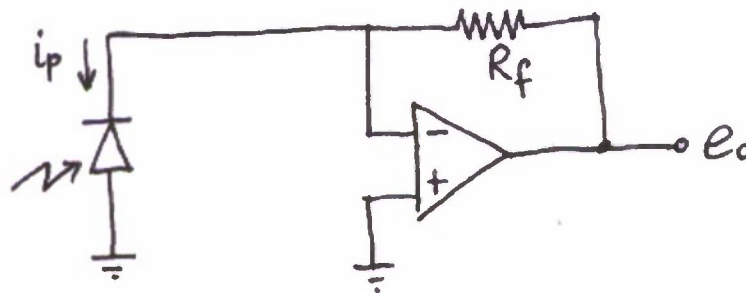


Figure 2. Basic photodiode transconductance amplifier

Because of the virtual ground at the op-amp's inverting input pin, the voltage across the diode is very small. This helps to ensure a large amplifier bandwidth by reducing currents through the diode capacitance C_D , thereby ensuring that almost all of the diode current passes through the feedback resistor R_f rather than through C_D .

Bandwidth can be further increased by decreasing the closed-loop gain of the op-amp connected to the diode. If this is done, the overall gain can be brought up to the desired value by using more than one stage of amplification, as illustrated in Figure 3.

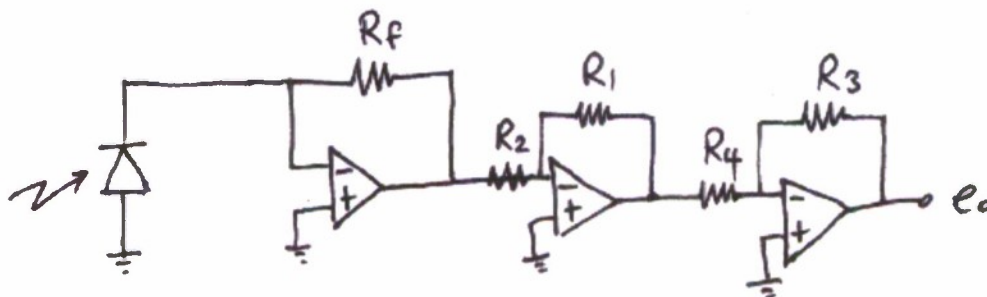


Figure 3. Three stage photodiode amplifier.

When used as a photodiode amplifier, the transconductance amplifier exhibits a complex noise behavior, in spite of the apparent simplicity of the basic circuit of Figure 2. The nature of this noise response and methods of reducing noise are presented in chapters 5 and 6 of reference [1]. The noise behavior of the photodiode amplifier has the following two undesirable properties that distinguish it from most other op-amp circuits:

1. There is “noise gain peaking” at high frequencies due to the interaction of parasitic capacitances within the amplifier. Above a certain frequency, the noise gain increases before eventually leveling off and then decreasing again once the op-amp’s open-loop gain roll-off is reached, as illustrated in Figure 4 below.
2. The circuit amplifies the signal with a lower bandwidth than that with which the noise is amplified.

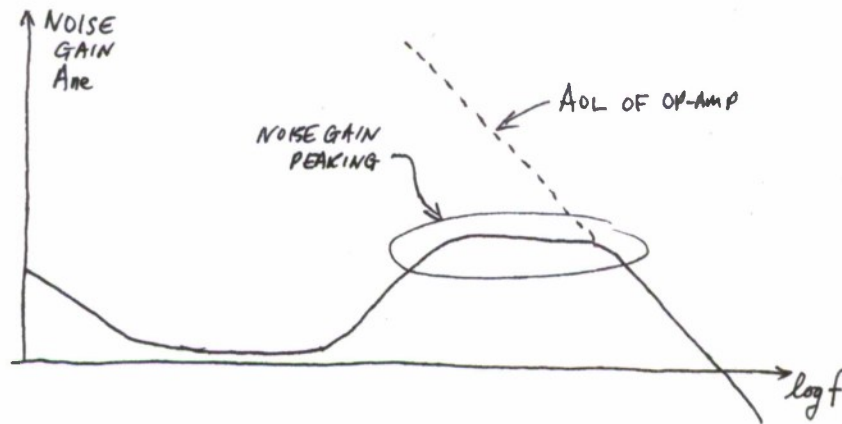


Figure 4. Photodiode amplifier noise gain, showing noise gain peaking.

This project is investigating several approaches to increasing the signal bandwidth of the amplifier, and limiting the adverse effects of noise caused by noise gain peaking and excessive noise-gain bandwidth.

II.2. Bootstrapping the photodiode

The signal voltage across the photodiode in the basic circuit of Figure 2 is very small, of order e_0/A_{OL} , where A_{OL} is the op-amp open-loop gain. However, our application makes use of a photodiode with a high capacitance (225pF) and requires a bandwidth of about 3 MHz. This is a stringent requirement to satisfy, and it was found that even the small e_0/A_{OL} signal voltage across the diode capacitance caused the bandwidth to be too low.

Bootstrapping reduces the voltage across the photodiode even further, by connecting a unity-gain buffer across it. The idea is illustrated in Figure 5, where an ideal unity-gain buffer is connected across the diode.

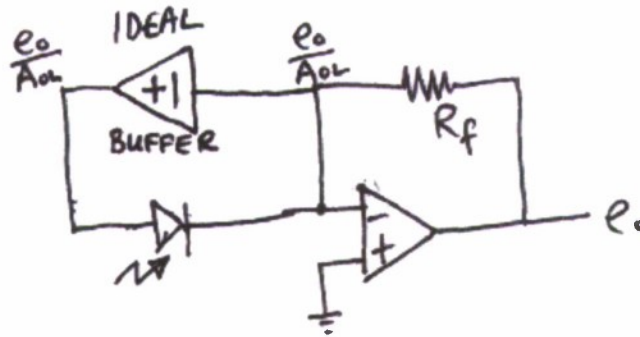


Figure 5. The bootstrapping concept.

The ideal buffer ensures that the voltage across the diode is exactly zero at all times, and of course this eliminates all influence upon the circuit by the diode capacitance C_D . This was verified by simulating the circuit of Figure 5 using a voltage-dependent voltage source for the ideal buffer.

In the real world, of course, an ideal buffer does not exist. For bootstrapping to be successful, the buffer must satisfy four stringent requirements:

1. low input capacitance (buffer input capacitance must be much less than photodiode capacitance)
2. low noise (buffer noise must be less than op-amp input noise)
3. wide bandwidth (buffer bandwidth must be much higher than op-amp bandwidth)
4. low output impedance

Figure 6 shows a modified version of the 3-stage circuit of Figure 3, where bootstrapping has been implemented using a fourth op-amp connected as a unity-gain follower.

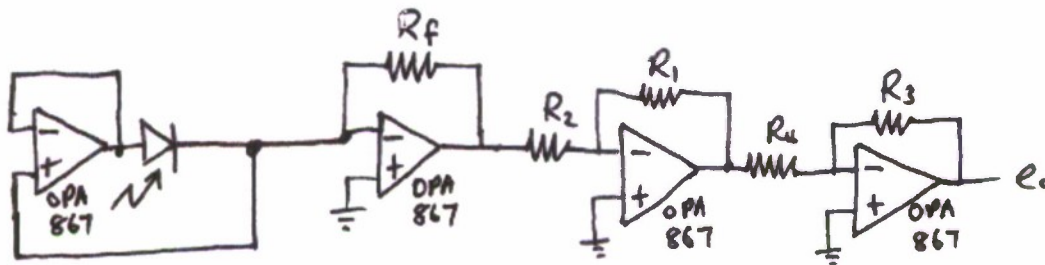


Figure 6. Bootstrapped three-stage photodiode amplifier using unity-gain op-amp buffer.

Simulation showed that the bandwidth of this amplifier did not increase to the extent anticipated. This was initially surprising, but it clearly demonstrated just how stringent the above 4 requirements upon the buffer actually are. Essentially, what was going wrong was that the buffer did not have a wide enough bandwidth in spite of the op-amp's large crossover frequency, because the crossover frequency of the OPA687 is not stable to low closed-loop gain.

The op-amp follower circuit was then replaced with a specialized unity-gain follower, the MAX4200, as shown in Figure 7.

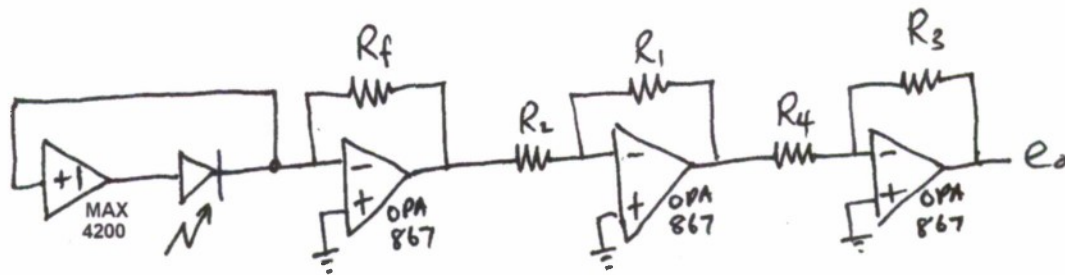


Figure 7. Bootstrapped photodiode amplifier using MAX4200 buffer.

Under simulation, the circuit of Figure 7 provided greatly improved bandwidth and lower noise as compared with Figure 3. This is to be expected, because the MAX4200 has 2pF input capacitance, low noise, 660 MHz bandwidth, and 8Ω output impedance, and therefore satisfies the four very stringent requirements listed earlier.

Another approach is to use a discrete circuit rather than an integrated circuit for the unity gain buffer. Shown in Figure 8 is a bootstrapped photodiode amplifier using a discrete unity gain buffer. The buffer consists of the three JFETs, one BJT and associated resistors.

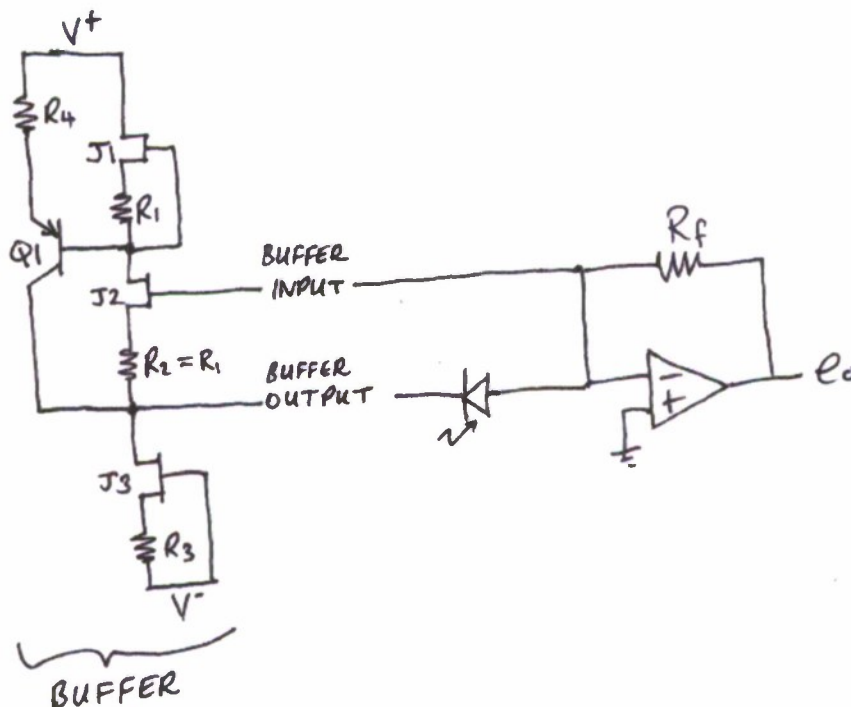


Figure 8. Bootstrapped photodiode amplifier using discrete buffer.

II.3. Approaches to reducing noise

The bootstrapped three-stage amplifier circuit of figure 7 has potential for further noise reduction because the problems of noise-gain peaking and inequality between signal and noise-gain bandwidth.

To reduce noise peaking: One way of reducing noise is to put a capacitance across the feedback resistor R_f of the transconductance amplification stage. This functions by reducing the magnitude of the noise-gain peaking, i.e. it reduces the height of the high-frequency “bump” in the noise gain curve of Figure 4.

To reduce noise-gain bandwidth: A pole in the signal gain response causes it to start rolling off at a lower frequency than the noise gain response. The result is that there is a range of frequencies where the op-amp is amplifying noise and not signal. This can be dealt with by reducing the open-loop gain of the op-amp so that the roll-off in open-loop response prevents the unnecessary amplification of noise within this range of frequencies.

II.4 Noise-gain reduction using a composite amplifier

Figure 9 shows a variation of the basic photodiode transconductance amplifier where a second op-amp A_2 is placed within the feedback loop in order to modify the open-loop response of op-amp A_1 . Examination of Figure 9 shows that the modified open-loop response has the following behavior:

1. At low frequencies, C_1 is open circuit, so that the full open-loop gain of A_2 is contributed to the composite amplifier.
2. At high frequencies, C_1 is short circuit, so that A_2 contributes a gain of R_2/R_1 to the composite amplifier. (By choosing $R_2 < R_1$, we ensure that this contribution is in fact an attenuation).

We see that the effect of including op-amp A_2 , we are reducing the open-loop gain of the composite amplifier for high frequencies. By appropriate choice of R_1 , R_2 , and C_1 , we can control the open-loop response such that the noise-gain bandwidth is made equal to the signal-gain bandwidth. Details are in reference [1], pages 117-118.

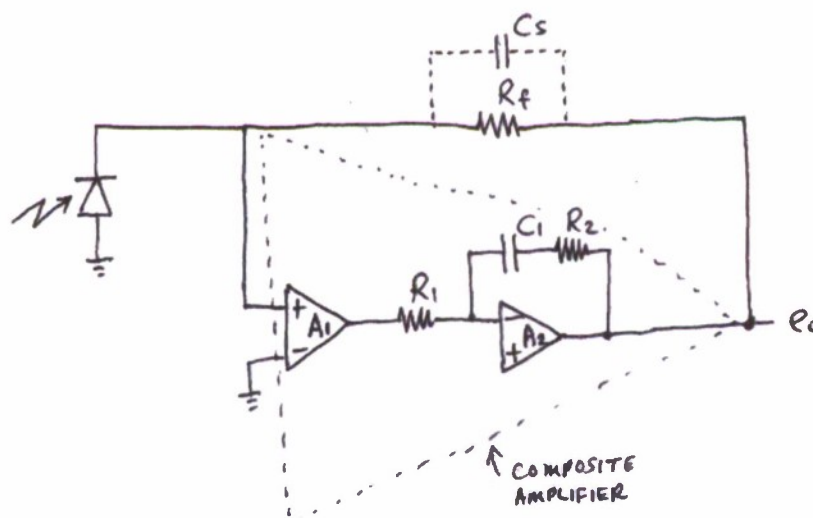


Figure 9. Noise-gain reduction using a composite amplifier.

II.5. Improving frequency response using negative capacitance

The primary factor that limits the frequency response of the system is the very high parasitic capacitance ($C_D = 225\text{pF}$) of the photodiode. The basic transimpedance circuit (Figure 2) and bootstrap circuit (Figure 5) are both designed with a view to ensuring that the signal voltage across the diode is made as small as possible, thereby limiting the ability of the diode parasitic capacitance to attenuate the signal.

An alternative approach would be to design a circuit that simulates a capacitance having a negative value of $C_N = -225\text{pF}$. Connecting this circuit in parallel with the photodiode, one would then have $C_{\text{total}} = C_D + C_N = 225\text{pF} + (-225\text{pF}) = 0$, thereby cancelling out the effect of the diode parasitic capacitance.

A negative capacitance can be simulated using a negative impedance converter (NIC) circuit, illustrated in Figure 8.

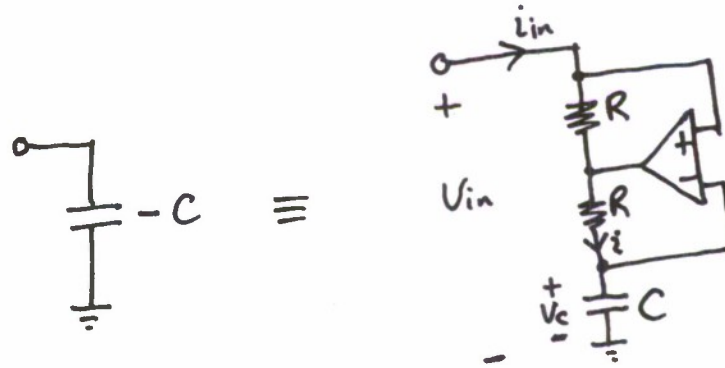


Figure 8. Using a negative impedance converter to simulate a negative capacitance.

Assuming that the op-amp is ideal, its two inputs will be at the same potential. Therefore, $i_m R + i R = 0$, which implies that $i = -i_m$. Also because of the virtual short-circuit, we have $v_C = v_m + 0 = v_m$. The capacitor obeys $v_C = i / sC$, so that the effective impedance looking into the NIC's terminal will be $Z_{in} = \frac{v_m}{i_m} = \frac{v_C}{-i} = \frac{1}{s(-C)}$ ohms. Therefore the circuit looks like a capacitance of $-C$ Farads.

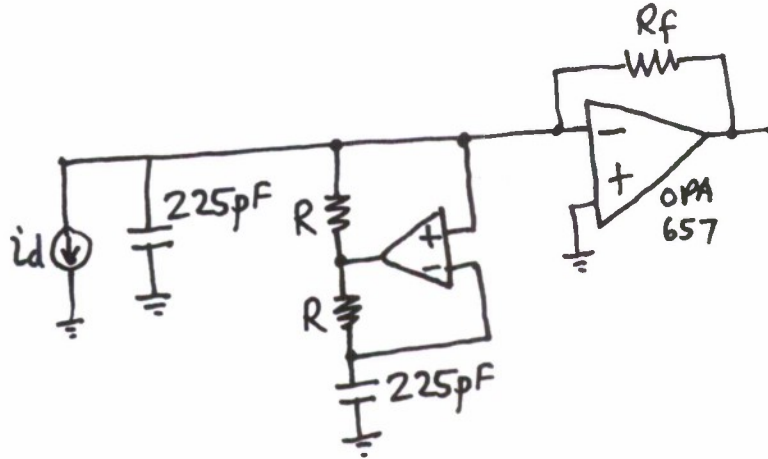


Figure 9. Basic photodiode amplifier, with diode capacitance cancelled using NIC.

Figure 9 shows the basic amplifier of Figure 2, modified to include a negative capacitance connected in parallel with the photodiode. This circuit was simulated, and was found to perform well if the NIC contained an ideal op-amp. Unfortunately, if the NIC contained any real op-amp (even one with the highest specifications available), then it was found that the simulation of negative capacitance failed at a frequency that was too low for the present application. The approach of using negative capacitance was therefore abandoned.

II.6. Two-transistor bootstrap circuit

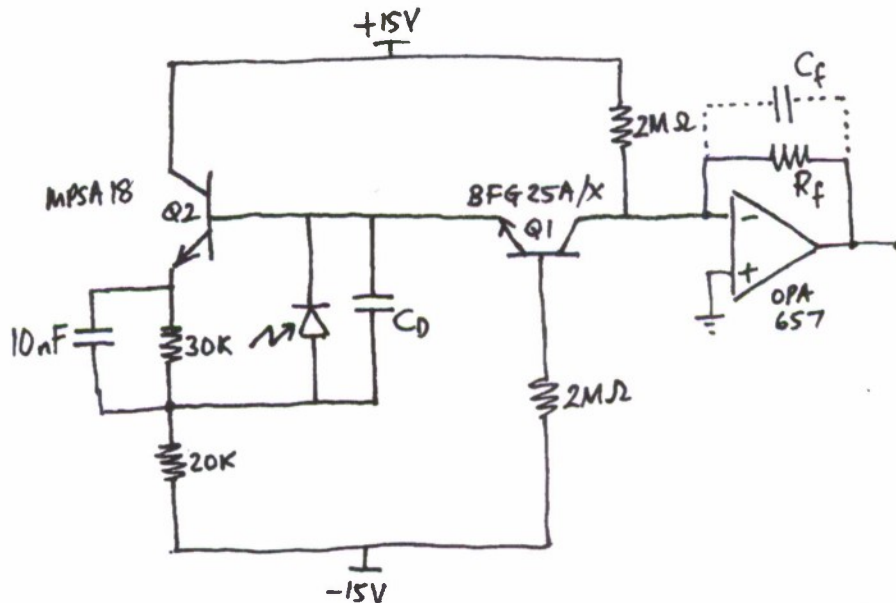


Figure 10. Photodiode amplifier, with two transistor bootstrap.

Figure 10 shows an amplifier in which the bootstrapping is achieved using a configuration of two transistors [3]. In this circuit, Q_2 keeps the voltage across the diode constant, while Q_1 provides current buffering.

Circuit analysis of the bootstrap portion of the circuit yields the following transfer function:

$$A_i(s) = \frac{i_{C1}}{i_D} = \frac{1}{1 + sC_D \left(1 + \frac{r_{\pi 1}}{\beta_1 R} \right) \left(R \parallel \frac{r_{\pi 2}}{\beta_2} \right)}$$

II.7. Noise performance comparison

The following three circuits were simulated in order to compare their noise performance:

- The two-transistor bootstrap circuit
- The bootstrap circuit using the MAX 4200 unity gain buffer
- The bootstrap circuit using the MAX 4200 unity gain buffer and a composite amplifier.

For convenience, the circuit diagrams are repeated in Figure 11. Their noise performance up to 10 MHz is illustrated in Figure 12.

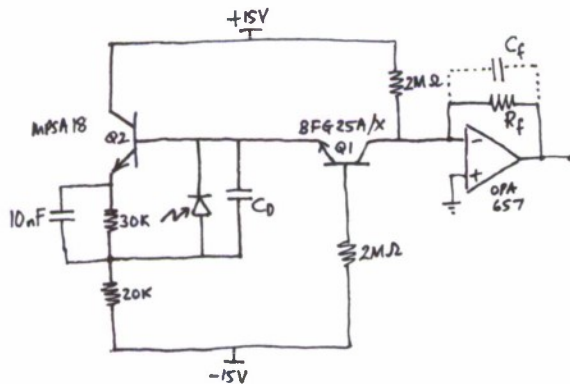


Figure 11 (a) Two-transistor bootstrap circuit

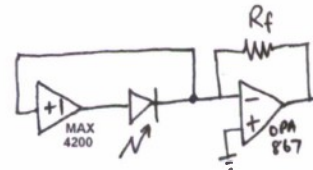


Figure 11 (b) Bootstrap circuit with MAX4200 buffer

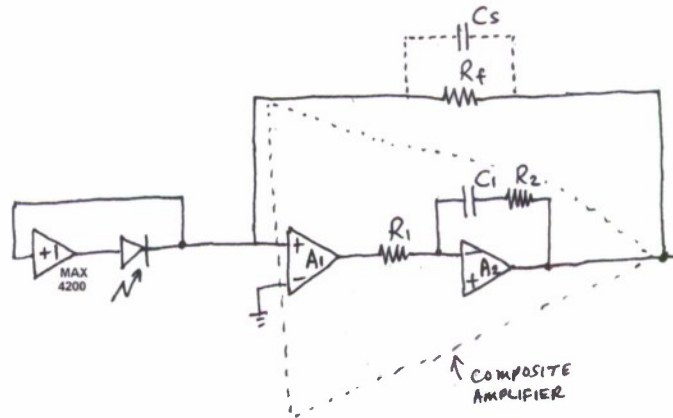


Figure 11 (c) Bootstrap with MAX4200 buffer and composite amplifier

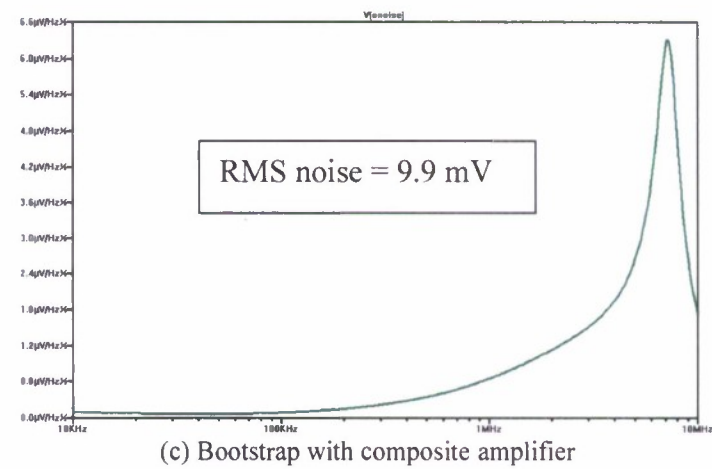
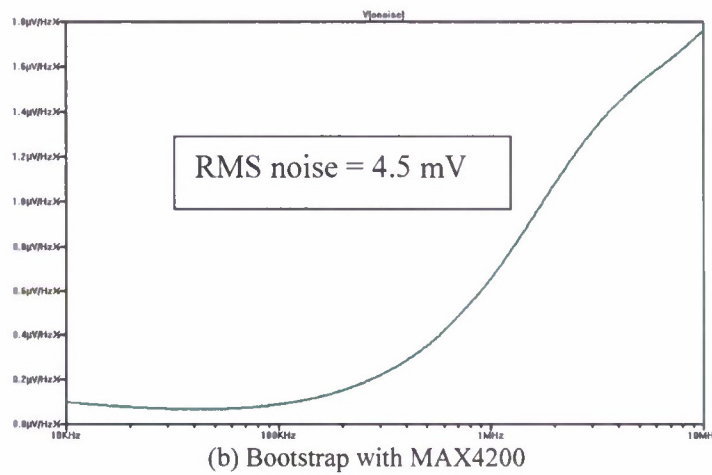
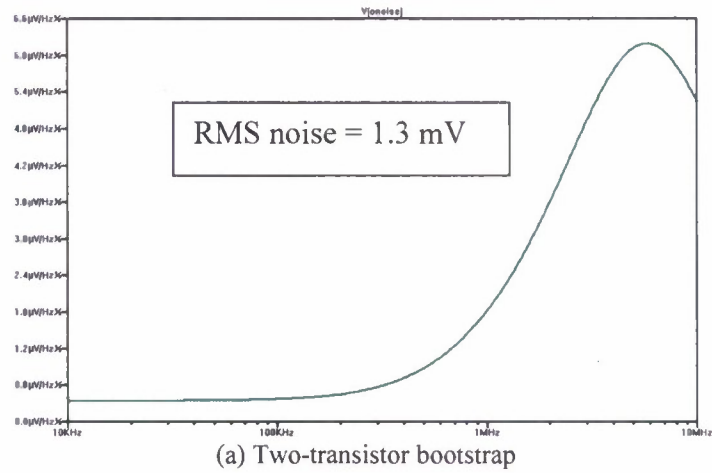
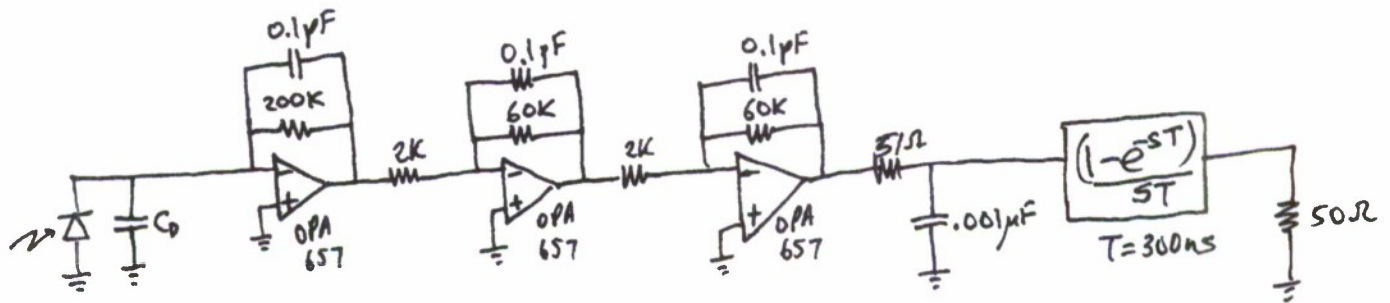


Figure 12. Noise performance results.

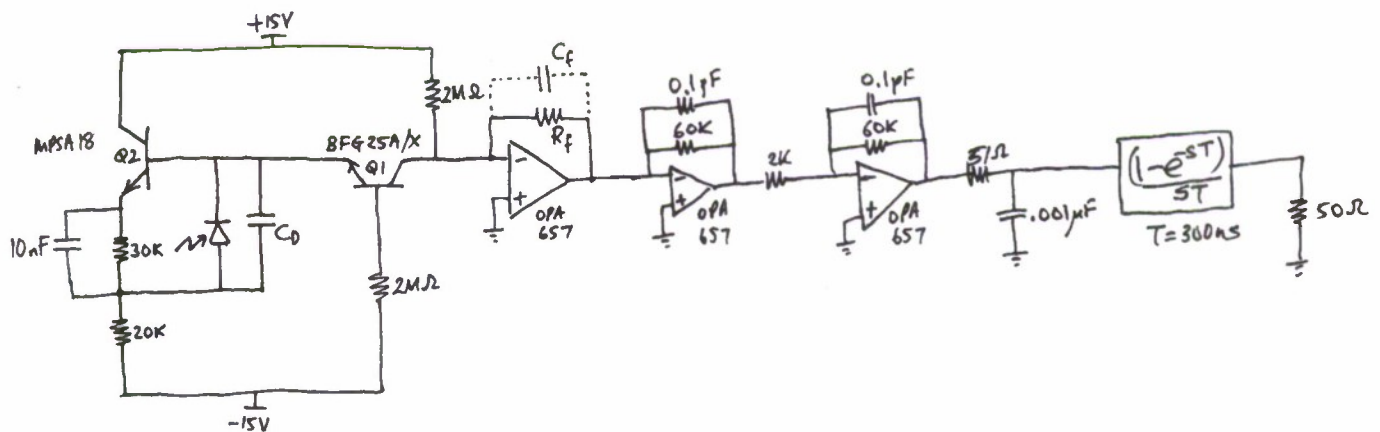
The simulations yielded overall RMS noise voltages of 1.3 mV, 4.5 mV, and 9.9 mV for circuits (a), (b), and (c) respectively. Circuit (a) exhibits clearly superior noise performance compared to the other two circuits. Therefore the two-transistor bootstrap approach was chosen.

II.8. Evaluation of chosen circuit

The two-transistor bootstrap circuit of Figure 10 was augmented with two further op-amp voltage gain stages, and was compared under simulation with the original three-stage circuit without bootstrap (Figure 3). The two circuits are illustrated in Figure 13.



(a) Original 3-stage amplifier



(b) Chosen 3-stage amplifier with 2-transistor bootstrap.

Figure 13. The two circuits whose performance is compared in Section III.4

The noise responses are shown in Figure 14, where it can be seen that the bootstrap circuit produces 330mV RMS noise, a considerable improvement over the 1870 mV for the original circuit.

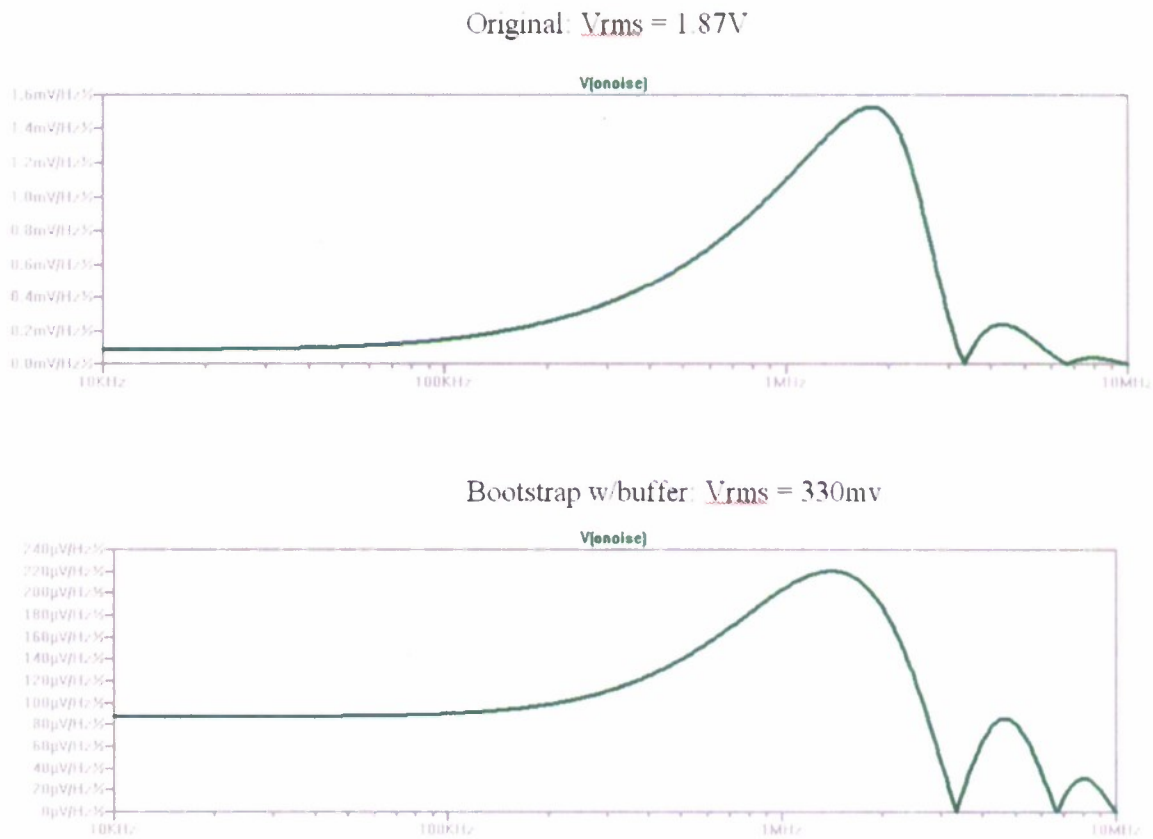


Figure 14. Noise performance of the circuits in Figure 13.

Figure 15 compares the signal gain frequency responses of the two circuits. Both circuits produce the same DC gain, but the bootstrap is very clearly superior, having a higher bandwidth (3.92 MHz versus 3 MHz) and a flat frequency response that does not show the undesirable peaking exhibited by the original circuit.

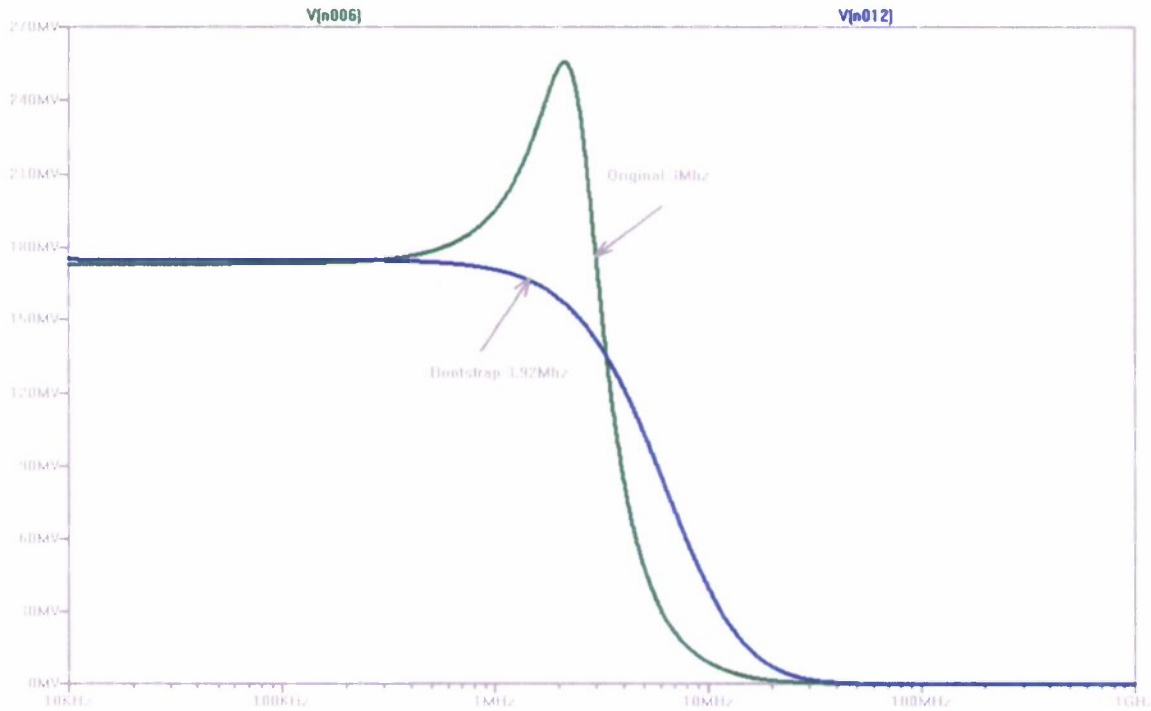


Figure 15. Signal frequency responses of the circuits of figure 13. Note the superiority of the blue curve representing the two transistor bootstrap circuit.

II.9. Work done after August 15, 2008.

The great bulk of the work for this grant was done Naval Surface Warfare Center in Dahlgren, VA, where the P.I. visited and worked full-time during the summer months of 2008 (May 22 to August 15). During the remainder of 2008, work continued on a part-time basis, and involved mostly the study of literature related to laser designation and tracking algorithms [3-11]. This was done with a view to prepare the P.I. for further work on MPLD systems.

III. References

1. Jerald Graeme, "Photodiode amplifiers – Op Amp Solutions", McGraw Hill 1996.
2. MAX4200 data sheet, Maxim Integrated Products, 120 San Gabriel Drive, Sunnyvale, CA 94086
3. Philip C.D. Hobbs, "Building Electro-Optical Systems", Wiley-Interscience, 2000.
4. Silvano Donati, "Photodetectors, circuits and applications", Prentice Hall 2000.

5. Dan Simon, "Optimal State Estimation", Wiley 2006.
6. Mark Johnson, "Photodetection and measurement: maximizing performance in optical systems", McGraw-Hill 2003.
7. J. H. Wilkinson, "The Algebraic Eigenvalue Problem", Clarendon Press, 1965.
8. R.A. Horn and C.R. Johnson, "Matrix Analysis", Cambridge University Press, 1999.
9. G.H. Golub and C.F. Van Loan, "Matrix Computations", Johns Hopkins University Press, 1996.
10. M.S. Grewal et. al., "Global Positioning Systems, Inertial Navigation, and Integration", Wiley 2007.
11. D.H. Titterton and J.L. Weston, "Strapdown Inertial Navigation Technology", AIAA 2005.

Acknowledgement:

Thanks are due to Ken Nichols for the plots of Figures 12, 14, and 15.